The effect of implantation, energy, and dose on extended defect formation for MeV phosphorus implanted silicon

Craig Jasper
Predictive Engineering Laboratory, Motorola, 2200 West Broadway Road, Mesa, Arizona 85202

Allen Hoover
Component Development Manufacturing Center, Motorola, 2200 West Broadway Road, Mesa, Arizona 85202

Kevin S. Jones
Department of Materials Science and Engineering, SWAMP Center, University of Florida, Gainesville, Florida 32611

(Received 9 June 1999; accepted for publication 31 August 1999)

The effect of dose and energy on postannealing defect formation, for high energy (MeV) phosphorus implanted into epitaxially grown silicon, has been studied by etch pits and transmission electron microscopy (TEM). The phosphorus dose was varied from 1×10^{13} to $5\times10^{14}\,\mathrm{cm}^{-2}$ and the energy was varied from 180 to 5000 keV. After implantation, the wafers were processed through subsequent annealing cycles which simulates a typical advanced complementary metal–oxide–semiconductor process to understand the formation of the defects in the near surface and projected range. For phosphorus energies above 500 keV, the threading dislocation density (TDD), increases dramatically with increasing dose from below the minimum detection limit ($5\times10^{3}\,\mathrm{cm}^{-2}$) at a dose of $1\times10^{13}\,\mathrm{cm}^{-2}$ to a maximum above $1\times10^{6}\,\mathrm{cm}^{-2}$ for a dose of $1\times10^{14}\,\mathrm{cm}^{-2}$. However, with further increases in dose, the TDD decreases back close to the minimum detection limit. Plan-view TEM suggests that with increasing dose, the formation of extended defects at the projected range reduces the TDD. For a fixed dose of $1\times10^{14}\,\mathrm{cm}^{-2}$, the TDD exhibits a superlinear increase of nearly 3 orders of magnitude as the implant energy is increased from 180 to 2000 keV. With further increases in implant energy, the TDD saturates at a value around $2\times10^{6}\,\mathrm{cm}^{-2}$. The marked effect of dose and energy on the TDD can be partially understood from homogeneous nucleation theory.
 [S0003-6951(99)05443-1]

High energy (MeV) implantation is rapidly being integrated into advanced complementary metal–oxide–semiconductor processes. These process steps include novel structures such as retrograde wells gettering implants, and buried layer formation.[1–3] A detailed understanding of the dopant diffusion and its interaction with process induced defects is critical for reliable device fabrication. The device performance and specifications demand certain species, projected ranges, and carrier concentration from the implantation process. However, even the smallest concentration of defects in the active device region can cause leakage and other device related problems.[4]

Understanding the unique material aspects of damage accumulation during very high energy implantation is critical in improving the performance of these new devices. The high energy (MeV) implantation process creates excess damage in the region near the projected range R_p of the implant that upon annealing contains a significant concentration of interstitials. Upon further annealing these interstitials evolve into extended defects (dislocation loops). The interaction of implantation and subsequent annealing conditions on defect formation has been reviewed by several groups.[5–10] It was found that for a boron implant at a dose of around $1\times10^{14}\,\mathrm{cm}^{-2}$ there is a peak in the density of threading dislocations that grows from the projected range to the surface.[10] These results were for boron implants at a single implant energy. This letter reports on similar experiments for phosphorus implants at a variety of energies and doses. The results suggest there also exists a maximum in threading dislocations as a function of dose and that the occurrence of this maximum is a strong function of implant energy.

Extended defect formation was studied for a range of doses and high energy (MeV) implant conditions followed by a low temperature anneal. Etch pit densities and plan-view and cross-sectional transmission electron microscopy (TEM) were used to characterize the type, depth, and concentration of dislocations in the material. The implants were carried out in 7 μm thick lightly doped ($1\times10^{15}\,\mathrm{cm}^{-3}$) P-type epitaxial silicon grown on (100) P+silicon. Phosphorus implant energies were varied from 180 to 5000 keV, at various doses, ranging from 1×10^{13} to $5\times10^{14}\,\mathrm{cm}^{-2}$. After implantation the samples were annealed at 800 °C for 90 min followed by a 550 °C anneal for 60 min and finally a 950 °C anneal for 10 min. Etch pit samples were produced using a Schimmel etch consisting of a 2:1 49% HF:1 M CrO_3 solution. An etch of 20 s was used.

To examine the projected range defects both plan-view and cross-sectional TEM was done on the samples after annealing. The plan-view samples were prethinned (when necessary) using chemical mechanical touch polishing (CMP) with a silica slurry, to position the peak of the projected range damage approximately 3000–4000 Å below the surface. A high resolution TEM operating at 200 kV was used to study the projected range defects. Micrographs were taken

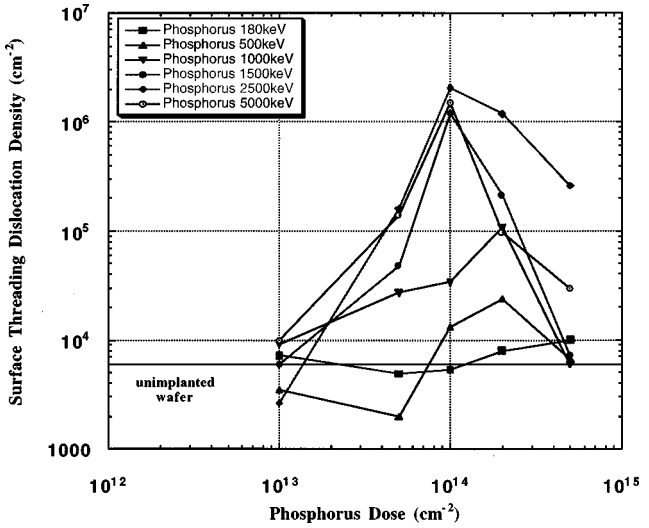

FIG. 1. Surface threading dislocation density for varying doses and energies for MeV phosphorus implanted samples. A peak threading dislocation density is shown to be at a dose of approximately $1\times10^{14}\,\mathrm{cm}^{-2}$.

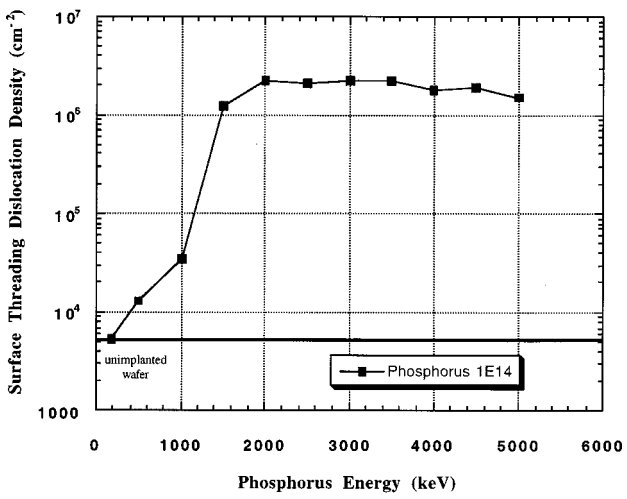

FIG. 2. Surface threading dislocation density for varying energies for phosphorus implanted samples. The peak surface threading dislocation density is not reached until an energy of greater than 1500 keV.

in bright field using $\mathbf{g}_{220}$ imaging conditions. These conditions allow one to observe defects as deep as 5000–10 000 Å. TEM of unimplanted control samples show that the CMP process does not introduce any observable defects.

Figure 1 shows the results of etch pit studies of the surface threading dislocation density for varying doses and energies for MeV phosphorus implanted samples. The background surface threading dislocation density (TDD) was obtained by etching an unimplanted sample to establish the number of dislocations for comparison. For all energies tested, at an implanted dose of $1\times10^{13}\,\mathrm{cm}^{-2}$ the TDD is similar to that of an unimplanted wafer of $5\times10^{3}\,\mathrm{cm}^{-2}$. This is the lower limit of TDD detection. Choosing an implant energy of 1500 keV as an example, when the implant dose was increased from 1×10^{13} to $5\times10^{13}\,\mathrm{cm}^{-2}$ the TDD increased to a threading density of $5\times10^{4}\,\mathrm{cm}^{-2}$. Upon increasing the dose to $1\times10^{14}\,\mathrm{cm}^{-2}$ the TDD reaches a peak threading density value of $2\times10^{6}\,\mathrm{cm}^{-2}$. Once the dose exceeds $1\times10^{14}\,\mathrm{cm}^{-2}$ the density of the threading dislocations rapidly decreases until a background value of $\leqslant1\times10^{4}\,\mathrm{cm}^{-2}$ is reached at a dose of $5\times10^{14}\,\mathrm{cm}^{-2}$. The effect of implant energy on this peak TDD at $1\times10^{14}\,\mathrm{cm}^{-2}$ is dramatic. At 180 keV the TDD for a dose of $1\times10^{14}\,\mathrm{cm}^{-2}$ is similar to that of an unimplanted sample. However, as the energy is increased in increments of 500 keV up to 1500 keV the TDD rapidly increases to a peak value of $2\times10^{6}\,\mathrm{cm}^{-2}$, which is over 2 orders of magnitude above the background level. This is illustrated in Fig. 2. At this dose ($1\times10^{14}\,\mathrm{cm}^{-2}$) the TDD saturates for energies between 1500 and 5000 keV.

To explain how the energy and dose affect the threading dislocation density it is necessary to understand the source of the threading dislocations and how these implant parameters affect the interstitial supersaturation that can lead to dislocation formation. It was recently shown that unfaulting of {311} defects can account for the formation of subamorphizing dislocations loops.[11] With increasing implant energy for doses $\leqslant1\times10^{14}\,\mathrm{cm}^{-2}$, the elongated shape of the dislocation loops observed by TEM is consistent with the threading dislocations arising from the unfaulting of long {311} defects (Fig. 3). This implies that understanding {311} nucleation is necessary for understanding threading dislocation density. The {311} defects are essentially precipitates of excess self interstitials. As such, if their formation is viewed as the homogeneous nucleation of a precipitate then the number of defects and their size is controlled by the supersaturation of excess self interstitials. For doses that are less than $1\times10^{14}\,\mathrm{cm}^{-2}$, at lower energies (<200 keV) the implant produces interstitial excesses, upon low temperature annealing, that mimic the dose.[12,13] At low energies (<200 keV) {311} defects form at doses as low as $1\times10^{13}\,\mathrm{cm}^{-2}$.[14] However, the dose needed to nucleate dislocation loops is approximately $2\times10^{14}\,\mathrm{cm}^{-2}$.[15] For doses below $2\times10^{14}\,\mathrm{cm}^{-2}$, this would imply very few threading dislocations form at the lowest energy studied and this is observed. However, as the energy increases the concentration of excess interstitials near the projected range increases because of the increased separation of Frenkel pairs.[16] This increase in interstitial concentration would increase the supersaturation of the interstitials. However, the straggle of the implant is also increasing which would tend to decrease the supersaturation of interstitials, so it is not clear which effect would dominate.

There is a second observation that may be important. We have observed by TEM that as the energy increases the average length of the {311} defects not parallel to the surface

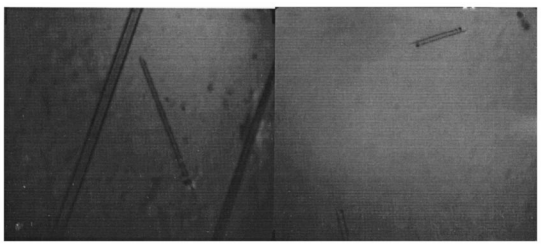

FIG. 3. Plan view TEMs of phosphorus implanted samples at a dose of $1\times10^{14}\,\mathrm{cm}^{-2}$. The micrographs show the presence of several threading dislocations at energies of 2500 and 5000 keV (TEM magnification 90 000×).

also increases. If the probability for a {311} defect unfaulting increases with increasing length, then increasing the implant energy would increase the concentration of {311}'s unfaulting into loops and thus increase the concentration of threading dislocations. There presumably would be some optimum dose for which the length of {311}s is at a maximum as a result of increasing the supersaturation of interstitials. Upon exceeding this dose, the supersaturation becomes higher and decreases the size of the critical nuclei for {311}s. This results in a rapid increase in the number of {311} defects and thus the average size becomes much smaller. If the defects are more numerous but smaller, then the threading dislocation density would decrease but the number of small loops at the projected range would increase. This indeed was observed by TEM for all implant energies and will be expanded upon in a future publication. This explains why the threading dislocation density decreases above the dose of $1\times10^{14}\,\mathrm{cm}^{-2}$.

Figure 3 shows plan-view TEM micrographs of phosphorus implanted samples at a dose of $1\times10^{14}\,\mathrm{cm}^{-2}$. The samples at 2500 and 5000 keV both have several threading dislocations present, as shown by the TEM view graphs. This threading dislocation evolution is difficult to predict and measure since it is near or below the detection limit of TEM. These TEMs are consistent with what we have seen from the surface threading dislocation density plots and other TEM micrographs.

Thus as suggested, there are probably several factors that contribute to the evolution of the threading dislocation density with increasing implant energy and dose, including changes in the number of excess interstitials and their distribution with depth. Another factor that could contribute to an increase in supersaturation with increasing energy is a decrease in surface recombination. However it was recently reported that there is no measurable influence of a surface on the formation of {311} defects for surfaces at least several thousand Å away.[17] It has been reported that extended defects are observed to form less than a few hundred Å to the surface.[18] Recently we have followed this with additional studies that show a negligible effect of the surface on the {311} formation at depths greater than several hundred Å. Thus, it would appear the surface plays a relatively minor role on the formation of {311} defects over the deep implants studied in this work. The effect of the distance to the surface for the formation of threading dislocations that reach the surface probably is significant. With increasing energy the dose of excess interstitials also increases as previously stated. These two effects may combine to result in the observed saturation in threading dislocation density shown in Fig. 2.

The effect of varying the implant energy and dose of high energy phosphorus implants on the threading dislocation density has been studied. For higher energy implants ($>$500 keV) the threading dislocation density increased with increasing dose to a maximum around $1\times10^{14}\,\mathrm{cm}^{-2}$. For higher doses the threading dislocation density decreases rapidly while the concentration of loops at the projected range increases. As a function of implant energy the threading dislocation density for $1\times10^{14}\,\mathrm{cm}^{-2}$ implants increases very rapidly, then saturates for implant energies $\geqslant$2 MeV. The trends in dose and energy can be qualitatively explained by viewing the system as a nucleation limited precipitation process involving self interstitials and estimating the effect of the processing conditions on the interstitial supersaturation.

The authors would like to thank the Implant group in Advanced Custom Technologies for the numerous hours that they have spent on preparing and running the many samples that it took to generate the data for this letter. The authors would also like to thank B.J., R.J., and S.J. for their assistance with the data analysis.

[1] H. Y. Lin and C. H. Ching, Nucl. Instrum. Methods Phys. Res. B **37/38**, 960 (1989).
[2] H. Wang, N. W. Cheung, P. K. Chu, J. Lin, and J. W. Mayer, Appl. Phys. Lett. **52**, 1023 (1988).
[3] J. O. Borland and R. Koelsch, Semicond. Sci. Technol. **36**, 28 (1993).
[4] J. Washburn, Defects Semicond. **2**, 209 (1980).
[5] M. Tamura, N. Natsuaki, Y. Wade, and E. Mitani, Nucl. Instrum. Methods Phys. Res. B **21**, 438 (1987).
[6] A. K. Rai, J. Baker, and D. C. Ingram, Appl. Phys. Lett. **51**, 172 (1987).
[7] H. Wong, N. W. Cheung, and S. S. Wang, Nucl. Instrum. Methods Phys. Res. B **37/38**, 970 (1989).
[8] M. Tamura, N. Natsuaki, Y. Wada, and E. Mitani, Nucl. Instrum. Methods Phys. Res. B **21**, 438 (1989).
[9] W. Skorupa, E. Wieser, R. Groetzschel, M. Posselt, H. Buecke, A. Armigliato, A. Garulli, A. Beyer, and W. Markgraf, Nucl. Instrum. Methods Phys. Res. B **19/20**, 335 (1987).
[10] J. Y. Cheng, D. J. Eaglesham, D. C. Jacobson, P. A. Stolk, J. L. Benton, and J. M. Poate, J. Appl. Phys. **80**, 2105 (1996).
[11] J. Li and K. S. Jones, Appl. Phys. Lett. **73**, 3748 (1998).
[12] M. D. Giles, J. Electrochem. Soc. **138**, 1160 (1991).
[13] D. J. Eaglesham, P. A. Stolk, H.-J. Gossmann, T. E. Haynes, and J. M. Poate, Nucl. Instrum. Methods Phys. Res. B **106**, 191 (1995).
[14] D. J. Eaglesham, P. A. Stolk, H.-J. Gossmann, and J. M. Poate, Appl. Phys. Lett. **65**, 2305 (1994).
[15] K. S. Jones, S. Prussin, and E. R. Weber, Appl. Phys. A: Solids Surf. **45**, 1 (1988).
[16] S. Coffa, V. Privitera, F. Priolo, S. Libertino, and G. Mannino, J. Appl. Phys. **81**, 1639 (1997).
[17] J.-H. Li, M. E. Law, C. Jasper, and K. S. Jones, Mater. Sci. Semicond. Process **1**, 99 (1998).
[18] A. Agarwal, T. E. Haynes, D. J. Eaglesham, H.-J. Gossman, D. C. Johnson, J. M. Poate, and Y. E. Erokhin, Appl. Phys. Lett. **70**, 3332 (1997).